Research Square

Preprints are preliminary reports that have not undergone peer review.
They should not be considered conclusive, used to inform clinical practice,
or referenced by the media as validated information.

3D Interconnected Hierarchically Porous Cellulose/Chitosan Composite Aerogels for Efficient Enzyme Immobilization and Enhanced Phytochemical Biotransformation

Xi Lin
Beijing Forestry University
Quan Zhou
Beijing Forestry University
Litao Wang
Beijing Forestry University
Zijing Zhao
Beijing Forestry University
Yujie Fu
yujie_fu@163.com
Beijing Forestry University

Research Article

Keywords: Microcrystalline cellulose, MCC/CS-GA aerogel, Enzyme immobilization, Biotransformation, Jujuboside B

Posted Date: November 16th, 2026

DOI: https://doi.org/10.21203/rs.3.rs-10315769/v1

License: This work is licensed under a Creative Commons Attribution 4.0 International License.
Read Full License

Additional Declarations: No competing interests reported.

3D Interconnected Hierarchically Porous Cellulose/Chitosan Composite Aerogels for Efficient Enzyme Immobilization and Enhanced Phytochemical Biotransformation

Xi Lin[a, b, c], Quan Zhou[a, b, c], Litao Wang [a, b, c], Zijing Zhao[a, b, c], Yujie Fu[a, b, c*]

[a] State Key Laboratory of Efficient Production of Forest Resources, Beijing Forestry University, 100083 Beijing, PR China.

[b] The College of Forestry, Beijing Forestry University, 100083 Beijing, PR China.

[c] Beijing Key Laboratory of Efficient Synthesis of Plant Secondary Metabolites, 100083 Beijing, PR China.

* Corresponding author.

Tel: +010-62336778

E-mail address: yujie_fu@163.com (Yujie Fu).

Highlight:

- Hierarchical porous MCC/CS-GA aerogel was fabricated *via* Schiff base crosslinking for *β*-Glucosidase immobilization.
- Porous microenvironments enhanced enzyme stability and catalytic performance.
- The immobilized system achieved 78.4% biotransformation efficiency of Jujuboside A.
- The biocatalyst retained 70.43% activity after six reuse cycles.

Abstract: Enzymes possess high catalytic efficiency and remarkable selectivity. Consequently, they have garnered increasing attention as sustainable biocatalysts for green biomanufacturing. However, limited operational stability, poor reusability, and difficult recovery during catalytic processes remain major barriers to their practical applications. As a result, enzyme immobilization has surfaced as a robust approach for enhancing enzyme stability and enabling repeated reuse. Developing suitable immobilization carriers capable of providing favorable catalytic microenvironments remains a critical challenge. Porous biobased carriers offer promising platforms for enzyme immobilization since their high specific surface area and interconnected porous architecture. Herein, a microcrystalline cellulose/chitosan composite aerogel (MCC/CS-GA) was fabricated through glutaraldehyde crosslinking and freeze-drying as a robust biomass-derived support for β-glucosidase (β-Glu) immobilization. The MCC/CS-GA-bound β-Glu had better pH tolerance and thermal stability than the free enzyme. And it kept good catalytic activity in harsh conditions. Furthermore, after being stored at 4 ℃ for 15 days, The anchored enzyme kept over 75% activity from the start, which indicates an improvement in storage stability.The MCC/CS-GA-immobilized β-Glu also enabled facile catalyst recovery and preserved 70.43% of its original activity after six cycles, indicating excellent operational durability. Furthermore, the biotransformation of Jujuboside A into Jujuboside B, which possesses a lower molecular weight and enhanced blood-brain barrier permeability relative to its precursor, achieved an efficiency of 78.4%, representing an approximately 8-fold enhancement compared with the native plant extract. Therefore, the MCC/CS-GA immobilization system facilitated efficient phytochemical biotransformation and may exhibit broader potential for biotransforming diverse phytoglycosides into bioactive aglycones.

Furthermore, the porous cellulose-based carrier provides a versatile platform for enzyme immobilization toward sustainable biocatalytic applications.

Keywords: Microcrystalline cellulose; MCC/CS-GA aerogel; Enzyme immobilization; Biotransformation; Jujuboside B.

1. Introduction

Aerogel, a solid nano-porous material characterized by a three-dimensional, is highly interconnected network architecture that contains a gaseous dispersed phase within its pores. Aerogel conferrings an ultrahigh specific surface area, elevated porosity, and inherent biocompatibility, which collectively endow it with exceptional physicochemical attributes(Ferreira-Gonçalves et al., 2021; Fu et al., 2025). However, conventional inorganic aerogels suffer from poor flexibility, while chemically synthesized aerogels face dual challenges of fossil resource depletion and environmental pollution(Shi et al., 2021). Accordingly, renewable biopolymers, notably cellulose and chitosan, have emerged as optimal precursors for bio-aerogel fabrication by virtue of their environmental benignity and complete biodegradability, aligning with green manufacturing paradigms(Ayazi et al., 2020; García-González et al., 2021). Chitosan (CS) with its molecular structure rich in amino and hydroxyl moieties, enables efficient enzyme loading via electrostatic interactions or chelation, yet its intrinsic drawbacks—including low surface area, weak mechanical strength, and poor acid resistance—severely impede practical applications(Paul et al., 2024). The incorporation of cellulose as a reinforcing phase can effectively compensate for these deficiencies, as exemplified by the stable porous network structure demonstrated in CS/cellulose nanofiber composite aerogels(Cao et al., 2024). Similarly, Zhu et al. designed a innovative chitosan-des lignin hybrid gel for the adsorption of methylene blue and Congo red.(Zhu et al., 2023). These studies collectively demonstrate that cellulose-reinforced chitosan-based aerogels represent promising green carriers, yet their potential for enzyme immobilization remains to be fully explored.

β-Glu specifically catalyzes the hydrolysis of glycosidic bonds, making it a biocatalyst of significant importance in the food, pharmaceutical, and bioenergy sectors(Planas, 2023). However, free enzymes suffer from intrinsic limitations for industrial applications, including high production costs, susceptibility to inactivation, and challenges in recovery and reusability(Maghraby et al., 2023). Immobilization technology has emerged as pivotal for overcoming these constraints by endowing enzymes with enhanced stability, reusability, and reaction controllability(Cavalcante et al., 2021). Precedents include the immobilization of xylanase on oxidized nanocellulose, achieving a substrate conversion rate of 31%(Katić et al., 2025). and *β*-Glu supported on cellulose microspheres, which catalyzed the transformation of polydatin to resveratrol with a 93% conversion efficiency(Zhang, Wan, Yao, Chen, Ju, Shuang, Fu, Chen, Zhao, et al., 2020). These examples underscore that the synergistic design of porous carriers and enzyme systems represents the central paradigm for enhancing biocatalytic performance. Aerogels, by virtue of their hierarchical pore architecture, can significantly enhance substrate mass transfer; For instance, Zhang et al. developed a laccase@COF aerogel to degrade emerging water pollutants; after seven reuse cycles, the material still retained 75.7% of its initial catalytic activity.(Xiya Zhang et al., 2024). Similarly, Wang et al. utilized an amino-functionalized lignin/cellulose nanofiber aerogel to immobilize decarboxylase, achieving a conversion rate of 76.2% after 7 reuse cycles(X. Wang et al., 2024). Evidently, aerogel-based enzyme immobilization technology has demonstrated remarkable advantages, yet the rational design of systems explicitly tailored for precise biotransformation of natural products warrants further in-depth investigation. Aerogel-based enzyme immobilization offers numerous advantages, and its application for the biotransformation of natural products merits further investigation.

Semen Ziziphi Spinosae, a traditional Chinese medicine with medicine-food homology, contains saponins (Jujuboside A and B) as its principal bioactive constituents, which exhibit sedative-hypnotic, anti-inflammatory, and neuroprotective activities(Xu et al., 2021). Jujuboside B demonstrates superior pharmacological efficacy compared to Jujuboside A, attributed to its lower molecular weight and enhanced blood-brain barrier permeability(J. Wang et al., 2024). However, the natural abundance of Jujuboside B is exceedingly low. *β*-Glu can specifically hydrolyze the C-3 glucose moiety of Jujuboside A, thereby enabling its targeted conversion to Jujuboside B and mimicking gut microbiota-mediated metabolic processes(Li et al., 2024). Based on this rationale, the construction of a *β*-Glu immobilization system employing MCC/CS-GA aerogel as the carrier holds promise for overcoming the industrial application bottlenecks of free enzymes while concurrently providing a green paradigm for the high-value conversion of natural products.

In this study, MCC/CS-GA aerogel was fabricated by crosslinking microcrystalline cellulose/chitosan with GA, followed by freeze-drying. *β*-Glu was immobilized onto the aerogel and employed for the biotransformation of Jujuboside A to Jujuboside B. Owing to its robust performance, this immobilization system serves as a promising candidate in the enzymatic valorization of various phytochemicals.

2. Materials and methods

2.1 Materials and Chemicals

β-Glu was acquired from Shanghai Yingxin Laboratory Equipment Co., Ltd. (China). Jujuboside A and Jujuboside B standards were obtained from Chengdu Nakeli Biotechnology Co., Ltd. (Chengdu, China). pNPG was supplied by Solarbio Science & Technology Co., Ltd. (China). Chitosan and GA were

procured from Macklin Biochemical Co., Ltd. (China), and microcrystalline cellulose was sourced from Yuanye Biotechnology Co., Ltd. (China). Hydrochloric acid was supplied by Aladdin Industrial Inc. (China), with *Semen Ziziphi Spinosae* obtained from Shandong, China.

2.2 Preparation of MCC/CS-GA Aerogel

A homogeneous blend of 2.5 wt.% chitosan solution and 3 wt.% microcrystalline cellulose (MCC) suspension was prepared at a 1:1 volumetric ratio under continuous stirring for 50 min to ensure complete dispersion. GA was then introduced as a crosslinking agent at varying concentrations (0.1–0.7 wt.%), producing crosslinked hydrogel precursors with tunable network densities. Subsequent freeze-drying of these precursors yielded aerogel materials with a corresponding compositional gradient.

2.3 Enzyme Immobilization on MCC/CS-GA Aerogel

For enzyme immobilization, 4 mg of lyophilized MCC/CS-GA aerogel was incubated with 100 μL of β-Glu solution (60 U) at 50℃ for 4 h under continuous agitation. The enzyme-loaded aerogel was subsequently rinsed with phosphate buffer (pH 5.5) to remove unbound enzyme. Protein loading was measured using the Bradford assay(Bradford, 1976). Briefly, after incubating aliquots of both the immobilized enzyme preparation and wash solution with Coomassie Brilliant Blue G-250 reagent at 37 ℃ for 30 min, and the absorbance was measured at 595 nm.

2.4 Characterization of MCC/CS-GA Aerogel

SEM (Regulus 8100, Tokyo, Japan) was used to see the shape of MCC/CS-GA aerogels. AFM (Bruker Multimode 8, Karlsruhe, Germany) was used to get the size of the aerogels after enzyme loading. The chemical groups were checked by FT-IR (Nicolet 6700, Madison, USA). BET (Kubo-X1000, Beijing, China) was used to measure the surface area and pore size. TGA (DTG-60, Kyoto, Japan) was used to

test the heat stability. XPS (K-Alpha, Thermo Scientific, USA) was used to look at the element make-up of the samples.

2.5 Enzyme Activity Determination and Kinetic Parameter Analysis

Enzyme activity was determined via the pNPG method(Norkrans, 1957). Briefly, 0.1 mg of the MCC/CS-GA aerogel immobilized with *β*-Glu was mixed with 0.5 mL of 5 mmol/L pNPG and 0.5 mL of phosphate buffer (pH 5.5), followed by incubation at 50°C for 30 min(Zhou et al., 2026). Afterwards, 2 mL of 1 mol/L Na_2CO_3 was added to quench the reaction, and the absorbance at 400 nm was recorded. All tests were run three times. And the mean values were got. One unit (U) was the amount of p-nitrophenol (mmol) made in one minute. And the specific activity was shown as U/mg. The top activity was set as 100%. And the other groups were compared to it.

To investigate the kinetic characteristics of free and bound *β*-Glu systems, the hydrolysis reaction of pNPG was monitored under optimized conditions, with the pNPG concentration in phosphate buffer varying from 2 to 20 mmol/L. The experimental data were then analyzed by nonlinear regression based on the Michaelis-Menten model, from which the Michaelis constant (Km) and maximum reaction rate (Vmax) were obtained.(Zhang, Wan, Yao, Chen, Ju, Shuang, Fu, Chen, Zhao, & Liu, 2020)

2.6 Stability Characteristics and Recyclable Performance Investigation

The enzymatic activity profiles of free and grafted *β*-Glu as a function of pH were assessed at 50°C within the pH interval of 4.0 to 6.5. Temperature-dependent catalytic activity was evaluated at pH 5.5 over 35–60°C. Storage stability was monitored at 4°C by periodically measuring residual activity. For reusability assessment, the immobilized enzyme-loaded aerogel was recovered after each reaction cycle

by washing with phosphate buffer to remove residual substrate, then transferred to a fresh substrate solution to initiate the subsequent cycle.

2.7 Biotransformation of Jujuboside A to Jujuboside B

To systematically optimize the ultrasonic extraction of *Semen Ziziphi Spinosae*, 0.1 g samples of powdered material was treated under varying conditions of ethanol strength(40–80%, v/v), ratio of liquid ratio (5:1–25:1 mL/g), extraction time (10–50 min), and temperature (20–60℃). The resulting extracts were obtained, filtered and stored at 4℃ before analysis. For the biotransformation of standard Jujuboside A, either *β*-Glu/MCC/CS-GA or free *β*-Glu was mixed with 50 μL of Jujuboside A solution, adjusted to pH 4.0–8.0, and incubated at 20–60℃ for 1–8 h with shaking. The reaction mixtures were passed passed through a 0.22 μm filter and then run on HPLC. For the biotransformation of Jujuboside A in the crude extract, 1 mg of immobilized *β*-Glu was put into 2 mL of the extract solution and incubated at 40℃ for 4 h, followed by identical filtration and HPLC analysis. Three replicates were done for each experiment.

3. Results and discussion

3.1 Synthesis and Optimization of MCC/CS-GA Composite Aerogel

The MCC/CS-GA aerogel was synthesized via a facile crosslinking and freeze-drying protocol, as illustrated in Fig. 1a. Initially, chitosan and microcrystalline cellulose were dispersed in deionized water under continuous agitation at 25℃ for 0.5 h to form a homogeneous co-gel precursor. Subsequently, GA was introduced as a crosslinking agent, and the mixture was agitated for an additional 5 min at 25℃ to facilitate Schiff base formation between the aldehyde groups of GA and the amino groups of chitosan. The resultant gel was then freeze-dried at -80℃for 24 h to yield the final MCC/CS-GA aerogel. The

crosslinking mechanism is depicted in Fig. 1b, wherein GA functions as a bifunctional crosslinker, establishing covalent linkages between chitosan chains through imine bond formation to reinforce the three-dimensional network architecture(Xin Zhang et al., 2024). To optimize the GA concentration, a series of aerogels were fabricated with GA concentrations ranging from 0.1% to 0.7% (w/v). As shown in Fig.1c, increasing the GA concentration progressively intensified the aerogel's coloration and mechanical rigidity. This phenomenon arises from enhanced crosslinking density, which promotes tighter molecular packing and modifies light scattering/absorption characteristics, resulting in deeper coloration(Phoungtawee et al., 2025). Concurrently, elevated crosslinking densities reduce pore dimensions and may induce partial pore closure, yielding a more compact and rigid structural network(Chen et al., 2000). When the GA content was 0.4%, the aerogel exhibited optimal properties and the highest measured enzyme activity. (Fig. 1d). Continuously increasing GA concentration can lead to excessive cross-linking, disrupting the normal spatial conformation of enzyme molecules and decreasing enzyme activity(Vazquez-Ortega et al., 2018). Therefore, 0.4% GA was determined to be the optimal concentration and used for subsequent research.

3.2 Morphological and Structural Characterization of MCC/CS-GA Aerogel

The MCC/CS-GA aerogel exhibits a hierarchical nanofibrillar architecture, as evidenced by SEM (Fig. 2a), which reveals an interconnected three-dimensional network with an average fiber diameter of 26.7 nm. This ultrafine fibrillar structure, coupled with the porous framework confirmed by AFM topography (Fig. 2b), which exhibits micron-scale surface roughness and height variations up to 5.0 μm, is crucial for providing a high-surface-area architecture and accessible diffusion pathways. The N_2 adsorption-desorption isotherm (Fig. 2c) displays a typical Type IV curve with a distinct H3 hysteresis

loop, a signature of mesoporous materials with slit-shaped pores, indicating that the crosslinking process preserves the porous structure, which is essential for mass transport and functional applications. And the BET surface area is 5.96 m^2/g, the overall pore volume is 0.022 cc/g, and the mean pore diameter is 3.63 nm. Thermal characterization demonstrates that glutaraldehyde crosslinking significantly enhances the thermal stability of the composite aerogel. TGA curves (Fig. 2d) reveal a three-stage decomposition pattern for both materials, with the MCC/CS-GA aerogel exhibiting a notably higher onset degradation temperature and a higher residual char yield than the uncrosslinked counterpart. The DTG profiles (Fig. 2e) further quantify this improvement, showing that the maximum decomposition rate temperature is shifted to higher values for the crosslinked sample, consistent with the formation of a more rigid molecular network that restricts thermal motion and delays cellulose chain scission. This enhanced thermal resistance is attributed to the stable imine linkages formed during the GA-mediated crosslinking reaction. The successful formation of Schiff base crosslinks is unequivocally confirmed by complementary spectroscopic analyses. FTIR spectra (Fig. 2f) of the MCC/CS-GA aerogel reveal a characteristic C=N stretching vibration at approximately 1655 cm^{-1}, a feature absent in both pristine MCC and the uncrosslinked MCC/CS aerogel, while simultaneously preserving the O–H (3400 cm^{-1}) and C–O (1050 cm^{-1}) bands of the polysaccharide backbone(Feng et al., 2021). High-resolution XPS N 1s spectra provide direct evidence of chemical transformation: the uncrosslinked MCC/CS aerogel exhibits two nitrogen environments at 398.99 eV (C–N=C) and 401.62 eV ($–NH_2$) (Fig. 2h), whereas the MCC/CS-GA aerogel (Fig. 2i) shows a dominant C–N=C peak shifted to lower binding energy (398.37 eV) with increased relative intensity, accompanied by a diminished and shifted –NH component (402.05 eV). This systematic decrease in free amino groups and concomitant increase in imine bonds

substantiates that glutaraldehyde efficiently crosslinks the chitosan amine moieties, creating a chemically stable hybrid network(Zhang et al., 2021).

3.3 Immobilization of Enzyme on MCC/CS-GA Aerogel

The immobilization of the enzyme onto the MCC/CS-GA aerogel was optimized through a systematic evaluation of key parameters, including initial enzyme concentration, enzyme loading rate, pH, and temperature. As shown in Fig. 3a, the enzyme loading exhibited a saturation curve, gradually increasing with initial enzyme concentration and plateauing at approximately 1.2 $U \cdot g^{-1}$ when the concentration exceeded 80 $U \cdot mL^{-1}$, indicating that the available binding sites on the aerogel matrix had reached saturation. Meanwhile, relative specific activity of the immobilized enzyme showed a distinct optimum, reaching approximately 95% at an initial enzyme concentration of 60 $U \cdot mL^{-1}$. Notably, when the concentration exceeded this optimal range, the relative activity gradually declined despite continued increases in protein loading. This phenomenon can be attributed to enzyme overcrowding on the support surface, which introduces diffusional limitations and leads to unfavorable molecular orientations, thereby diminishing substrate accessibility and specific activity(Serial et al., 2026). The immobilization efficiency, defined as the percentage of enzyme activity attached to the support matrix relative to the initial activity, was also evaluated as a function of initial enzyme concentration (Fig. 3b). The immobilization rate reached a maximum of 78% at an initial enzyme loading of 60·U mL^{-1}, as the limited number of reactive aldehyde groups on the aerogel surface became saturated at high enzyme loadings, leading to reduced binding yields(Agustian & Hermida, 2019).

The catalytic performance of the immobilized enzyme under different pH conditions is shown in Fig. 3c. At pH 5.0, the free enzyme had its best activity. But at pH 4.0 and 6.5, it had below 40% activity.

On the other hand, the immobilized enzyme demonstrated a significantly broader pH tolerance, maintaining over 80% relative activity across the entire examined pH range (4.0–6.5), with the optimal pH shifted to 5.0-5.5. This enhanced pH tolerance likely arises from the protective microenvironment within the aerogel pores and the stabilizing effect of covalent binding, which buffers the enzyme against external pH fluctuations. Thermal stability profiles further highlighted the advantages of immobilization (Fig. 3d). The free enzyme displayed maximum activity at 45–50℃, with activity sharply diminishing above 55℃, retaining less than 40% activity at 60℃. Conversely, the immobilized enzyme exhibited a broader optimal temperature range (50–55 ℃) and superior thermal stability, maintaining over 70% of its maximum activity even at 60 ℃. This improvement in thermal performance is attributed to the structural rigidification of the enzyme molecule upon covalent binding to the aerogel scaffold, which restricts conformational flexibility and thereby impedes thermal denaturation.

3.4 Kinetic Properties, Storage Stability, and Reusability of Enzyme Immobilized on MCC/CS-GA Aerogel

The Michaelis–Menten parameters derived from Lineweaver–Burk plots (Table 1) revealed that the immobilized enzyme exhibited a K_m value of 15.153 ± 44.352 mmol·L^{-1}, which was nearly identical to that of the free enzyme (15.017 ± 43.726 mmol·L^{-1}). This negligible difference indicates that no big change was seen in the enzyme's substrate affinity or binding after fixing. Similarly, the V_{max} values of the free and immobilized enzymes were comparable (6.952 ± 10.679 vs. 6.952 ± 10.773 μmol·L^{-1}·min^{-1}), suggesting that the inherent mass-transfer limitations of the aerogel's porous matrix were minimal and the intrinsic catalytic turnover rate was largely preserved(Bakar et al., 2024).

As illustrated in Fig. 4a, A 15-day storage test at 4 ℃ was done to check the enzyme's long-term stability. In contrast, the residual activity of the free enzyme declined rapidly, with merely 35–40 % of its starting activity left after 12 days. Unlike that, the MCC/CS-GA-bound enzyme exhibited remarkable stability, maintaining over 85 % of its initial activity during the same period. And operational stability was assessed through repeated batch catalytic cycles (Fig. 4b).The supported enzyme had approximately 95 % of its original activity after the first cycle, with a progressive decrement observed in subsequent runs. After five consecutive cycles, the biocatalyst maintained roughly 65–70 % of its original activity, demonstrating good reusability and mechanical robustness of the MCC/CS-GA support.

3.5 Biotransformation of Jujuboside A to Jujuboside B

First, the biotransformation of the standard Jujuboside A was carried out. As shown in Fig. S1, the optimal conditions for Jujuboside A biotransformation were determined as substrate concentration of 0.064 μmol, pH 5, temperature of 30℃, and reaction time of 1 d, which subsequently provided a basis for the conversion of Jujuboside A from extracts. Extraction of Jujuboside A from *Ziziphi Spinosi Semen* was subsequently optimized (Fig. S3), with the yield of Jujuboside A serving as the evaluation index. Key parameters, including solvent type, solid-to-liquid ratio, temperature, time, and extraction cycles, were systematically examined. Fig. 5 presents the HPLC chromatograms and concentration profiles of Jujuboside A and Jujuboside B before and after biotransformation catalyzed by *β*-Glu immobilized on MCC/CS-GA aerogel. Before enzymatic conversion, the chromatogram exhibited a predominant peak at a retention time of 12.3 min, corresponding to Jujuboside A with an initial concentration of 1.85 mmol·L^{-1}. The peak for Jujuboside B (retention time 8.7 min) was negligible (0.08 mmol·L^{-1}), confirming that minimal non-enzymatic hydrolysis occurred under the reaction conditions.

Following incubation with the immobilized enzyme at 50 ℃ for 4 h, the chromatogram revealed a substantial decrease in the Jujuboside A peak area (78.5% reduction), corresponding to a residual concentration of 0.40 mmol·L^{-1}. Concurrently, the Jujuboside B peak increased markedly, attaining a final concentration of 1.42 mmol·L^{-1}. This transformation corresponded to a molar yield of 78.4% with a selectivity exceeding 95%, demonstrating that the immobilized *β*-Glu efficiently catalyzed the regioselective cleavage of the terminal glucose moiety from Jujuboside A without significant side reactions.

The high conversion efficiency, coupled with retention of catalytic specificity, collectively confirms that the MCC/CS-GA aerogel provides an optimal microenvironment for preserving enzyme function during biotransformation. These results validate the practical applicability of the carrier-bound enzyme for sustainable making of Jujuboside B.

4. Conclusion

Herein, a hierarchically porous microcrystalline cellulose/chitosan composite aerogel (MCC/CS-GA) was successfully fabricated *via* glutaraldehyde-mediated crosslinking and freeze-drying as a robust biomass-derived platform for *β*-glu immobilization. The three-dimensional porous architecture, characterized by high specific surface area, dual-scale porosity, and abundant reactive functionalities, provided a favorable catalytic microenvironment for enzyme anchoring and substrate diffusion while preserving enzymatic activity. Stable Schiff base linkages enabled effective enzyme immobilization and contributed to enhanced operational performance. Compared with the native enzyme, the enzyme-loaded aerogel exhibited improved pH tolerance, thermal stability, storage stability, and reusability, preserving more than 85% of its starting activity after 15 days of storage

and approximately 70% activity after repeated operation cycles. Furthermore, the immobilized system achieved efficient biotransformation of Jujuboside A with 78.4%. The MCC/CS-GA immobilization platform demonstrated promising potential for biotransformation of glycosidic phytoconstituents and may provide a versatile biomass-derived strategy for sustainable biocatalysis and natural product modification.

Authorship contribution statement

Xi Lin: Writing – original draft, Conceptualization, Methodology, Data curation. Quan Zhou: Investigation, Methodology. Zijing Zhao: Writing – review & editing. Quan Zhou: Methodology. Xi Lin: Writing – review & editing. Litao Wang – review & editing. Litao Wang and Yujie Fu: Supervision, Writing – review & editing, Funding acquisition.

Declaration of Competing Interest

The authors declare that they have no known competing financial interests or personal relationships that could have influenced the work reported in this paper.

Data availability

Data will be made available on request.

Acknowledgments

This work got support from the following: National Natural Science Foundation of China (32271805), S&T Program of Xiongan New Area (XA202501102004K), 5·5 Engineering Research & Innovation Team Project of Beijing Forestry University (BLRC2023A01), and R&D Program of Beijing Municipal Education Commission (KM202410016011).

References

Agustian J, Hermida L(2019) Mesostructured cellular foam MCF-(9.2T-3D) silica as support for free α-amylase in liquefaction of tapioca starch. *IOP Conference Series: Materials Science and Engineering*, *509*(1), 012059.https://doi.org/10.1088/1757-899X/509/1/012059

Ayazi H et al(2020) Graphene aerogel nanoparticles for in-situ loading/pH sensitive releasing anticancer drugs. *Colloids and Surfaces B: Biointerfaces*, *186*, 110712.https://doi.org/10.1016/j.colsurfb.2019.110712

Bakar B et al(2024) Horseradish Peroxidase Immobilized onto Mesoporous Magnetic Hybrid Nanoflowers for Enzymatic Decolorization of Textile Dyes: A Highly Robust Bioreactor and Boosted Enzyme Stability. *ACS Omega*, *9*(23), 24558-24573.https://doi.org/10.1021/acsomega.4c00703

Bradford M M(1976) A rapid and sensitive method for the quantitation of microgram quantities of protein utilizing the principle of protein-dye binding. *Analytical Biochemistry*, *72*(1), 248-254.https://doi.org/10.1016/0003-2697(76)90527-3

Cao Y et al(2024) Preparation of chitosan/cellulose nanofibril composite aerogel and its adsorption performance for Cu(II)-MO binary pollutant. *International Journal of Biological Macromolecules*, *281*, 136418.https://doi.org/10.1016/j.ijbiomac.2024.136418

Cavalcante F T T et al(2021) Current Status and Future Perspectives of Supports and Protocols for Enzyme Immobilization. *Catalysts*, *11*(10). 10.3390/catal11101222.

Chen X et al(2000) Influence of crosslinking agent content on structure and properties of glutaraldehyde crosslinked chitosan membranes. *Acta Chimica Sinica*, *58*(12), 1654-1659.https://doi.org/10.61558/2993-074X.2961

Feng L et al(2021) Preparation of a rice straw-based green separation layer for efficient and persistent oil-in-water emulsion separation. *Journal of Hazardous Materials*, *415*, 125594.https://doi.org/10.1016/j.jhazmat.2021.125594

Ferreira-Gonçalves T et al(2021) Safety and efficacy assessment of aerogels for biomedical applications. *Biomedicine & Pharmacotherapy*, *144*, 112356.https://doi.org/10.1016/j.biopha.2021.112356

Fu Y et al(2025) Advance and perspective of carbon-based aerogels and their composites. *Chemical Engineering Journal*, *519*, 165304.https://doi.org/10.1016/j.cej.2025.165304

García-González C A et al(2021) Aerogels in drug delivery: From design to application. *Journal of Controlled Release*, *332*, 40-63.https://doi.org/10.1016/j.jconrel.2021.02.012

Katić K et al(2025) Biotransformation of xylan isolated from sunflower meal into xylo-oligosaccharides using endo-xylanase immobilized on oxidized nanocellulose. *Molecular Catalysis*, *585*, 115340.https://doi.org/10.1016/j.mcat.2025.115340

Li Y et al(2024) Research progress on biotransformation of saponins from traditional Chinese

medicine *Chinese Traditional and Herbal Drugs*, *February Vol. 55*.https://doi.org/10.7501/j.issn.0253-2670.2024.03.029

Maghraby Y R et al(2023) Enzyme Immobilization Technologies and Industrial Applications. *ACS Omega*, *8*(6), 5184-5196.10.1021/acsomega.2c07560

Norkrans B(1957) Studies of β-glucoside-and Cellulose Splitting Enzymes from Polyporus annosus Fr. *Physiologia Plantarum*, *10*(1),

Paul J et al(2024) Chitosan-based aerogels: A new paradigm of advanced green materials for remediation of contaminated water. *Carbohydrate Polymers*, *338*, 122198.https://doi.org/10.1016/j.carbpol.2024.122198

Phoungtawee P et al(2025) Spatiotemporal Retention of Structural Color and Induced Stiffening in Crosslinked Hydroxypropyl Cellulose Beads. *Macromolecular Rapid Communications*, *46*(5), 2400755.https://doi.org/10.1002/marc.202400755

Planas A(2023) Chapter 2 - Glycoside hydrolases: Mechanisms, specificities, and engineering. In Goyal, A Sharma, K (Eds.), *Glycoside Hydrolases* (pp. 25-53).https://doi.org/10.1016/B978-0-323-91805-3.00011-3

Serial M R et al(2026) A novel method for quantifying enzyme immobilization in porous carriers using simple NMR relaxometry. *Biochemical Engineering Journal*, *225*, 109909.https://doi.org/10.1016/j.bej.2025.109909

Shi W et al(2021) Preparation of aerogel beads and microspheres based on chitosan and cellulose for drug delivery: A review. *International Journal of Biological Macromolecules*, *170*, 751-767.https://doi.org/10.1016/j.ijbiomac.2020.12.214

Vazquez-Ortega P G et al(2018) Stabilization of dimeric β-glucosidase from Aspergillus niger via glutaraldehyde immobilization under different conditions. *Enzyme and Microbial Technology*, *110*, 38-45.https://doi.org/10.1016/j.enzmictec.2017.12.007

Wang J et al(2024) Study on the neuroprotective and sedative effects of the combination of jujuboside B and spinosin from Ziziphi Spinosae Semen. *Journal of Functional Foods*, *119*, 106274.https://doi.org/10.1016/j.jff.2024.106274

Wang X et al(2024) A pushed biosynthesis of 2,6-dihydroxybenzoic acid by the recombinant 2,3-dihydroxybenzoic acid decarboxylase immobilized on novel amino-modified lignin-containing cellulose nanocrystal aerogel. *Bioresource Technology*, *394*, 130218.https://doi.org/10.1016/j.biortech.2023.130218

Xu X et al(2021) Development of the general chapters of the Chinese Pharmacopoeia 2020 edition: A review. *Journal of Pharmaceutical Analysis*, *11*(4), 398-404.https://doi.org/10.1016/j.jpha.2021.05.001

Zhang D-Y et al(2020) Fabrication of three-dimensional porous cellulose microsphere bioreactor for biotransformation of polydatin to resveratrol from Polygonum cuspidatum Siebold & Zucc. *Industrial Crops and Products*, *144*, 112029.https://doi.org/10.1016/j.indcrop.2019.112029

Zhang D-Y et al(2020) Fabrication of three-dimensional porous cellulose microsphere bioreactor for biotransformation of polydatin to resveratrol from Polygonum cuspidatum Siebold & Zucc. *Industrial Crops and Products*, *144*, 112029.https://doi.org/10.1016/j.indcrop.2019.112029

Zhang M et al(2021) Anisotropic cellulose nanofiber/chitosan aerogel with thermal management and oil absorption properties. *Carbohydrate Polymers*, *264*, 118033.https://doi.org/10.1016/j.carbpol.2021.118033

Zhang X et al(2024) A flexible, thermal-insulating, and fire-resistant bagasse-derived cellulose aerogel prepared via a refrigerator freezing combined ambient pressure drying technique. *Chemical Engineering Journal*, *498*, 155466.https://doi.org/10.1016/j.cej.2024.155466

Zhang X et al(2024) Multi-enzyme-immobilized robust self-floating covalent organic framework/chitosan aerogels for the efficient remediation of emerging pollutants in water. *Journal*

of Environmental Chemical Engineering, *12*(6), 114791.https://doi.org/10.1016/j.jece.2024.114791

Zhou Q et al(2026) Bamboo-Inspired bionic microfluidic Reactor: Construction and application for industrial Biocatalysis. *Bioresource Technology*, *457*, 135013.https://doi.org/10.1016/j.biortech.2026.135013

Zhu Y et al(2023) Preparation of DES lignin-chitosan aerogel and its adsorption performance for dyes, catechin and epicatechin. *International Journal of Biological Macromolecules*, *247*, 125761.https://doi.org/10.1016/j.ijbiomac.2023.125761

Figure Captions

Fig. 1. (a) the process flow for preparing MCC/CS-GA aerogel through freeze-drying, (b) the crosslinking mechanism of MCC/CS-GA aerogel, (c) a physical comparison diagram of the effects of different concentrations of GA on the aerogel, and (d) the determination of the effect of aerogels prepared with different concentrations of GA on enzyme activity.

Fig. 2. (a) Scanning electron microscope (SEM) of MCC/CS-GA aerogel; (b) Atomic force microscopy (AFM) of MCC/CS-GA aerogel ; (c) N_2 adsorption-desorption isotherm and pore size distribution of MCC/CS-GA aerogel; (d) Thermogravimetric analysis (TGA) of MCC/CS aerogel and MCC/CS-GA aerogel; (e)Differential thermogravimetric (DTG) of MCC/CS aerogel and MCC/CS-GA aerogel; (f) Fourier-transform infrared spectroscopy (FTIR) of MCC, CS, MCC/CS aerogel and MCC/CS-GA aerogel; (g) X-ray photoelectron spectroscopy (XPS) of MCC/CS aerogel and MCC/CS-GA aerogel; (h) XPS N 1s spectrum of MCC/CS aerogel;

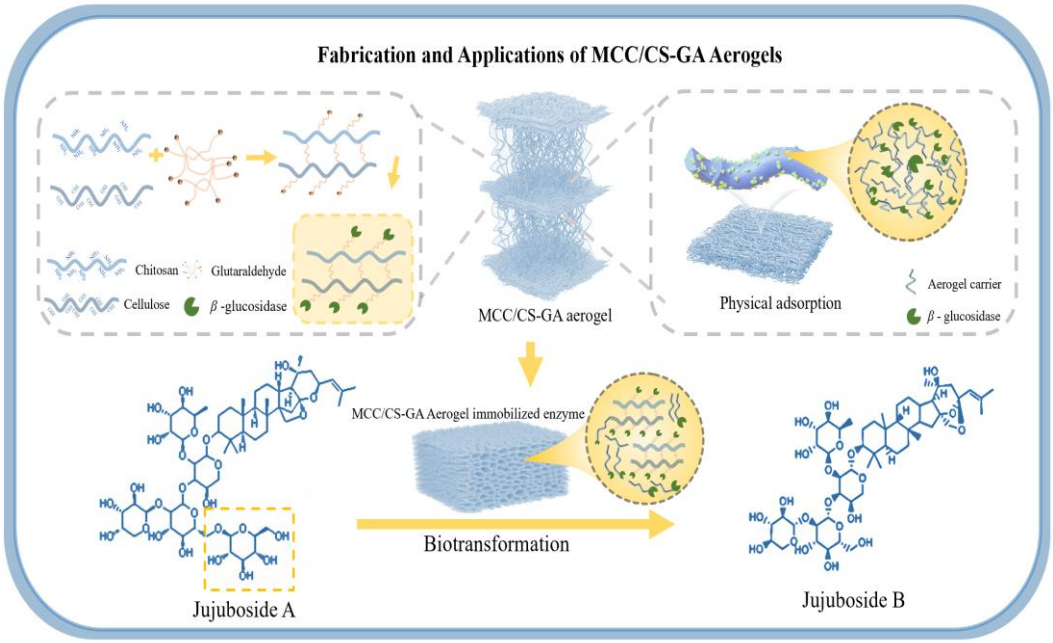
(i) XPS N 1s spectrum of MCC/CS-GA aerogel.

Fig. 3. (a) Enzyme loading and relative enzyme activity under different initial enzyme concentrations. Relative enzyme activity under different reaction conditions; (b) Changes in enzyme immobilization rate under different initial enzyme concentrations;(c) pH; (d) temperature.

Fig. 4. (a) Storage stability of immobilized enzymes; (b) Reusability test of MCC/CS-GA Aerogel

Fig. 5. Chromatograms and concentrations of Jujuboside A and Jujuboside B before and after biotransformation catalyzed by MCC/CS-GA aerogel immobilized enzyme.

Graphical Abstract:



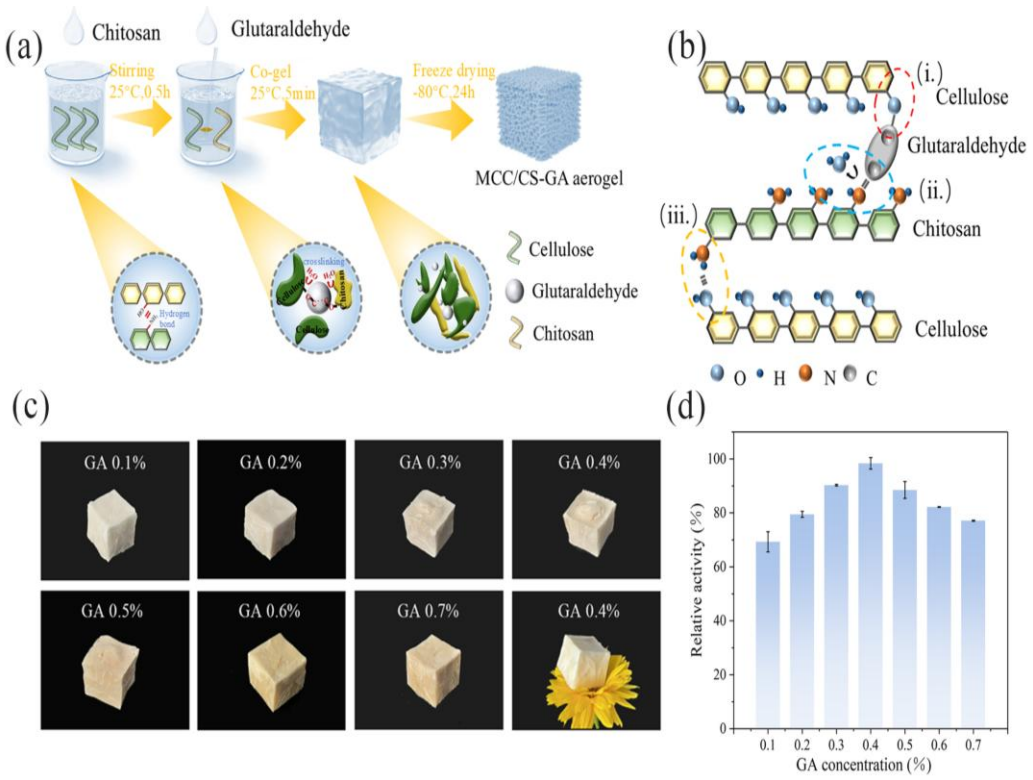


Fig. 1. (a) the process flow for preparing MCC/CS-GA aerogel through freeze-drying, (b) the crosslinking mechanism of MCC/CS-GA aerogel, (c) a physical comparison diagram of the effects of different concentrations of GA on the aerogel, and (d) the determination of the effect of aerogels prepared with different concentrations of GA on enzyme activity.

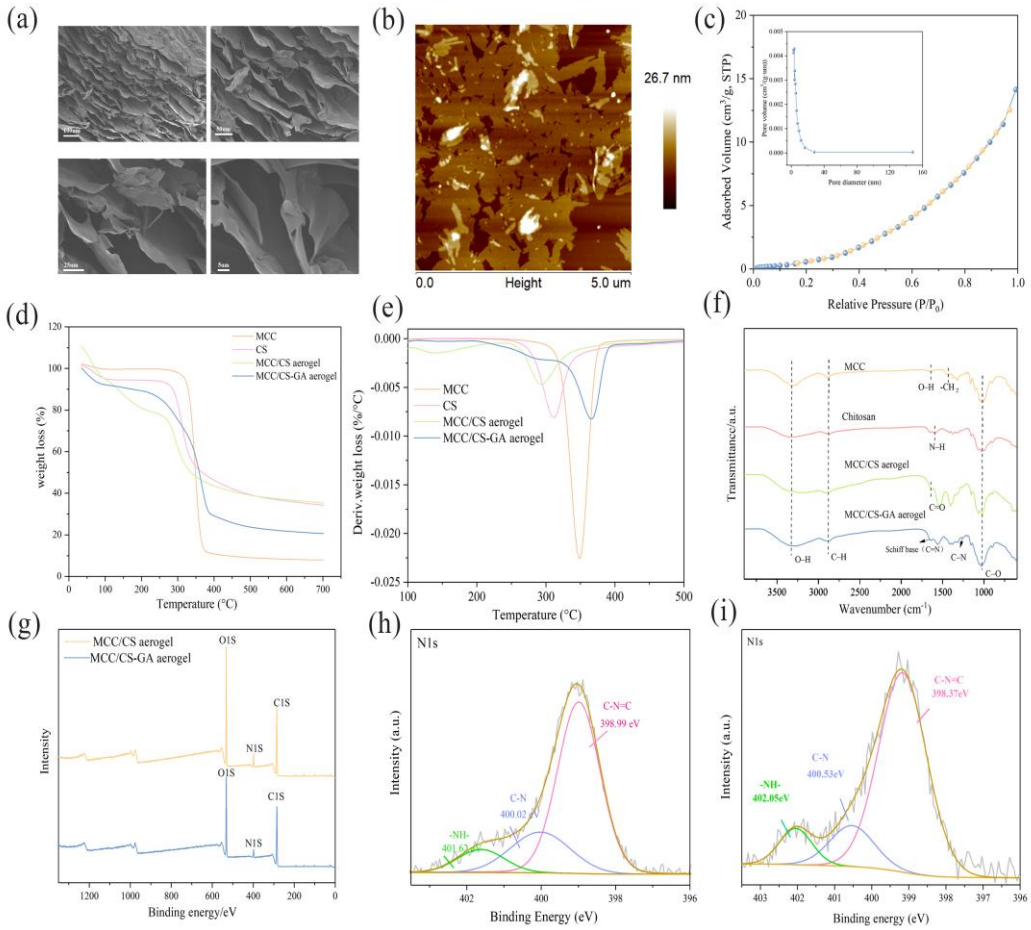


Fig. 2. (a) Scanning electron microscopy (SEM) images of MCC/CS-GA aerogel at the same location under different magnifications; (b) Atomic force microscopy (AFM) of MCC/CS-GA aerogel ; (c) N_2 adsorption-desorption isotherm and pore size distribution of MCC/CS-GA aerogel; (d) Thermogravimetric analysis (TGA) of MCC/CS aerogel and MCC/CS-GA aerogel; (e)Differential thermogravimetric (DTG) of MCC/CS aerogel and MCC/CS-GA aerogel; (f) Fourier-transform infrared spectroscopy (FTIR) of MCC, CS, MCC/CS aerogel and MCC/CS-GA aerogel; (g) X-ray photoelectron spectroscopy (XPS) of MCC/CS aerogel and MCC/CS-GA aerogel; (h) XPS N 1s spectrum of MCC/CS aerogel; (i) XPS N 1s spectrum of MCC/CS-GA aerogel.

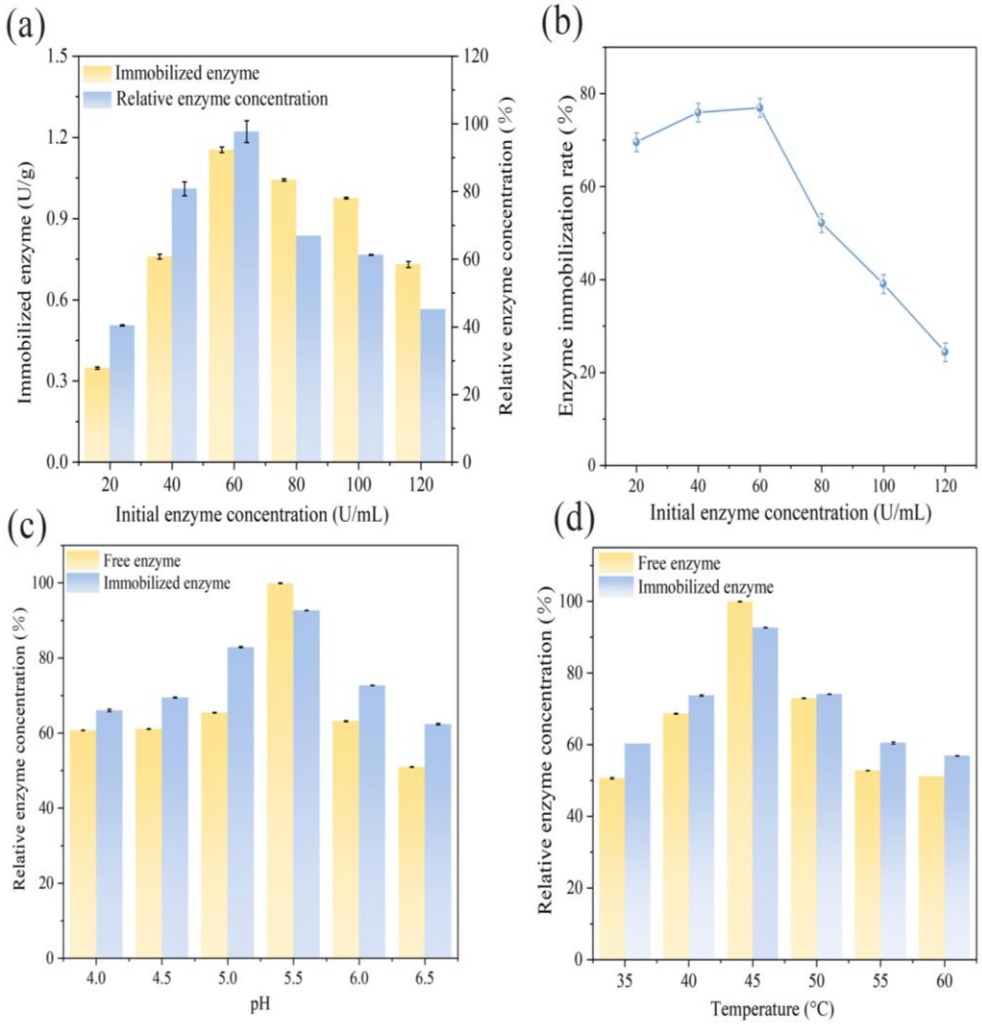


Fig. 3. (a) Enzyme loading and relative enzyme activity under different initial enzyme concentrations. Relative enzyme activity under different reaction conditions; (b) Changes in enzyme immobilization rate under different initial enzyme concentrations; Relative enzyme activity under different reaction conditions: (c) pH; (d) temperature.

Fig. 4. (a) Storage stability of immobilized enzymes; (b) Reusability test of MCC/CS-GA Aerogel

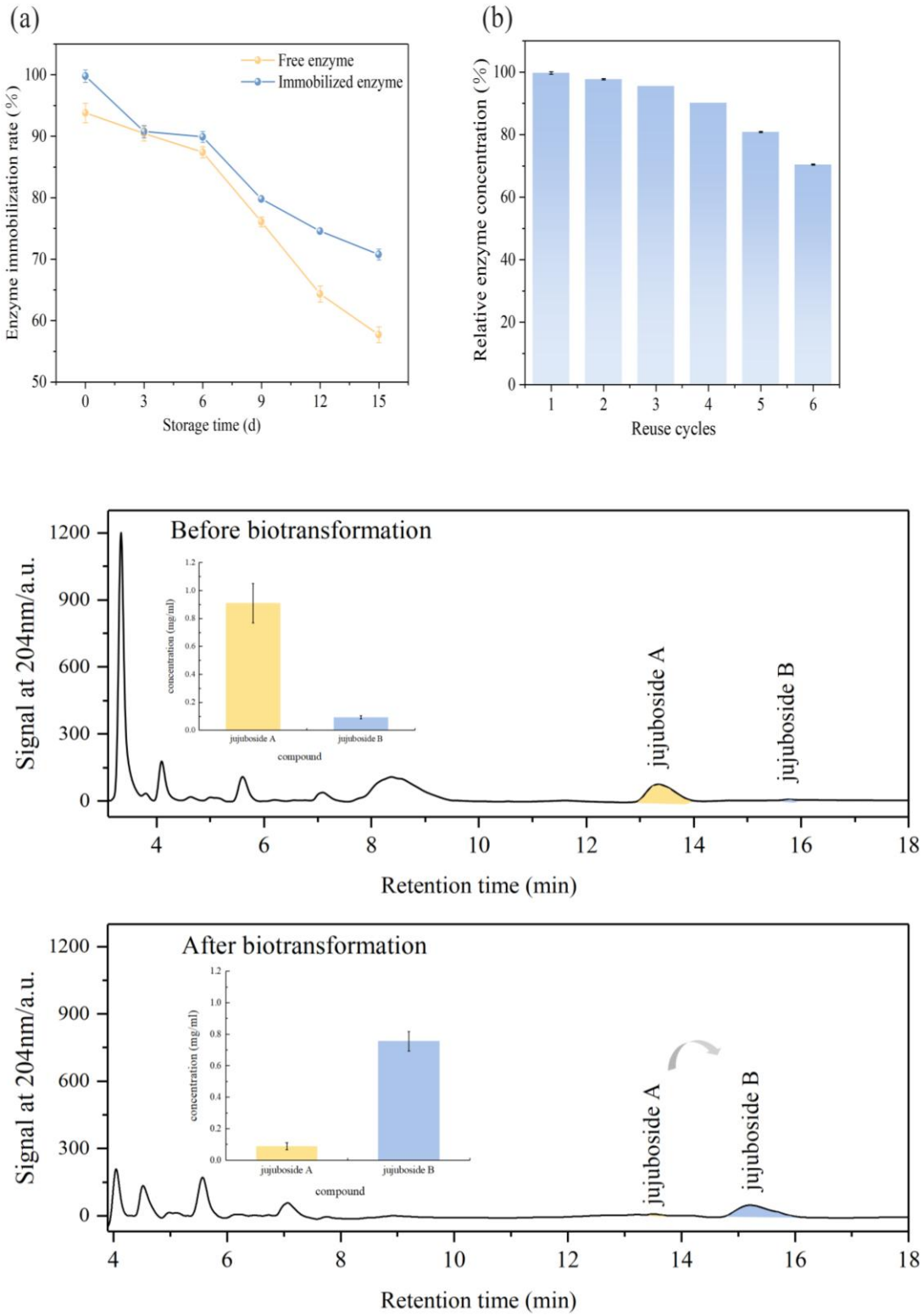


Fig. 5. Chromatograms and concentrations of Jujuboside A and Jujuboside B before and after biotransformation catalyzed by MCC/CS-GA aerogel immobilized enzyme.

Table 1. Michaelis-Menten equation of free enzyme and microreactors loaded with enzymes.

Biocatalyst	K_m **(mmol/L)**	V_{max} **(μmol/L·min^{-1})**
Free enzyme	15.017 ± 43.726	6.952 ± 10.679
Immobilized enzyme	15.153 ± 44.352	6.952 ± 10.773

Notes: K_m, Michaelis constant; V_{max}, maximum reaction velocity.

Supplementary Files

This is a list of supplementary files associated with this preprint. Click to download.

- Supplementaryinformation.docx